Short-circuit photocurrent in epitaxial lead zirconate-titanate thin films

L. Pintilie[a)]
Max Planck Institute of Microstructure Physics, Weinberg 2, 06120 Halle, Germany and NIMP, P.O. Box MG-7, Magurele, 077125 Bucharest, Romania

I. Vrejoiu, G. Le Rhun, and M. Alexe
Max Planck Institute of Microstructure Physics, Weinberg 2, 06120 Halle, Germany

(Received 28 August 2006; accepted 30 December 2006; published online 27 March 2007)

Photovoltaic properties of the metal-ferroelectric-metal structures, having $SrRuO_3$ metal oxide electrodes and $Pb(Zr,Ti)O_3$ (PZT) as ferroelectric layer, are investigated by the short-circuit photocurrent (SC-PHC) in the 200–800 nm wavelength domain. The band-gap dependence on the Zr content was determined from the spectral distribution of the SC-PHC signal. It was found that the band-gap value increases linearly with the Zr content, from about 3.9 eV to about 4.4 eV. It is shown that the sign and the magnitude of the signal depend on the internal bias and on the spontaneous polarization direction and value. The photocurrent describes a hysteresis loop similar to that of the ferroelectric polarization and can be used as a nondestructive readout of the nonvolatile memories based on PZT films. The existence of a significant SC-PHC signal at wavelengths corresponding to subgap energies is attributed to the presence of charged, deep levels in the forbidden band. It is also shown that the epitaxial PZT films have the potential for solid-state UV detectors, with current responsivity as high as 1 mA/W. The results are not entirely consistent with a bulk photovoltaic effect and are discussed in the frame of a Schottky barrier model for the metal-ferroelectric interface. © *2007 American Institute of Physics*. [DOI: 10.1063/1.2560217]

I. INTRODUCTION

Photoelectric properties of the lead zirconate-titanate (PZT) thin films were less investigated than their electric, ferroelectric, or piezoelectric properties. Generically, the photoelectric effect represents generation of an electric signal when the sample is illuminated with light with an appropriate wavelength.[1] Special care should be given to ferroelectric materials. The photoelectric signal must not be confused with the pyroelectric signal given by the well known pyroelectric effect, which in certain conditions might occur by illumination of a ferroelectric sample.[2] The photoelectric signal occurs only by photon generation of charge carriers at illumination with wavelengths in the ultraviolet-visible (UV-Vis) domain,[3–5] whereas pyroelectric signal occurs only due to the temperature variation of polarization and usually at wavelengths corresponding to the infrared (IR) domain. Two main differences are between the two signals: (i) pyroelectric signal is not due to generation of free carriers within the material,[6–8] and (ii) the pyroelectric signal occurs only in modulated light, while the photoelectric one occurs both under continuous and modulated illuminations.[9,10]

Historically, the bulk photovoltaic effect was the photoelectriclike phenomena observed in ferroelectric single crystals and ceramics such as $BaTiO_3$, $LiTaO_3$, and $LiNbO_3$.[11,12] It is worth noting that these materials also show a significant photorefractive effect.[12,13] Bulk photovoltaic effect consists in the generation of large voltages under homogeneous illumination with UV light. These voltages are usually much larger than the band gap of the material, which is in the range of 3–4 eV for the ferroelectric oxides with perovskite structure.[14,15] The main problem was to explain the presence of a short-circuit current under illumination. This cannot be generated without the presence of an internal electric field. Therefore, the existence of an internal electric field parallel to the ferroelectric polarization was assumed. Several theories were developed to explain this effect.[16,17] In general, it was assumed that the bulk photovoltaic effect in ferroelectrics has a different origin other than the standard photovoltaic effect in Schottky or *p-n* junctions. Eventually, serial connection of several junctions was assumed to explain the large photovoltages obtained in bulk ferroelectric ceramics.[18–20] Moreover, the effect of the UV radiation on the polarization hysteresis and fatigue was also studied. It was found that UV light illumination helps the polarization restoration after severe fatigue in polycrystalline PZT films.[21–23] This was explained by generation of additional mobile carriers which might play a significant role in a rapid compensation of the polarization charges and by the "erasing" of the charge defects that can act as pinning centers for the ferroelectric domains.

As we have already emphasized, the origin of the short-circuit photocurrent (PHC) in PZT films sandwiched between metal electrodes, i.e., metal-ferroelectric-metal (MFM) structures, is not yet clarified. Additionally, spectral distribution and the dependence of the PHC on the magnitude and orientation of the ferroelectric polarization were never in depth investigated. Relatively few studies were reported on generation of photocurrents under UV illumination of the MFM structures.[24–26] It was even proposed to use these currents as a nondestructive readout of the nonvolatile memories based on ferroelectric PZT.[27] PHC was measured not only at wavelengths corresponding to fundamental ab-

[a)]Electronic mail: pintilie@mpi-halle.mpg.de

sorption, i.e., below 400 nm,[24] but also at wavelengths below the band gap, e.g., 532 nm, which hints at the presence of impurity levels in the PZT forbidden band.[28] It was observed that the PHC can describe a hysteresis, suggesting its direct connection with the ferroelectric polarization, but no further studies were made to clarify the phenomena.[29]

The lack of consistent studies on photoelectric properties of the PZT thin films could be attributed to the fact that, in most cases, polycrystalline films were investigated. Polycrystalline films are defective systems which usually make difficult extraction of reliable photoelectric signals, due to destructive effects of the grain boundaries, which might act as traps for photogenerated carriers. Therefore, reliable studies must be performed on epitaxial films, with structural quality as close as possible to single crystal.

The present paper will show and analyze photoelectric measurements performed on high-quality epitaxial PZT thin films with various Zr/Ti ratios. Photocurrent signal generation is explained by the presence of the Schottky barriers at the PZT-electrode interfaces, and it will be shown that changes produced at the interfaces by the polarization switching are responsible for the change in the photocurrent sign. The spectral distribution of the PHC is carefully analyzed and it is shown to contain two components given by band-to-band and impurity absorptions. The band-gap value is extracted for PZT epitaxial films with different compositions and is compared with other reports. Also, the PHC dependencies on the thickness, polarization magnitude, and orientation are discussed, as well as the retention of the PHC sign in open- and short-circuit conditions. It is shown that the PHC can be used to probe the polarization state and the presence of imprint fields.

II. SAMPLE PREPARATION AND EXPERIMENTAL METHODS

PZT films were prepared by pulsed laser deposition (PLD) on $SrTiO_3$ (STO) substrates. First, an epitaxial layer of $SrRuO_3$ (SRO), acting as bottom electrode and as template for the growth of the PZT film, was deposited. Then PZT films with four different Zr/Ti ratios: 20/80, 40/60, 60/40, and 80/20 were deposited. The MFM structure was completed by the deposition of the top electrodes through a shadow mask. These were from SRO, deposited by PLD at room temperature, followed by a sputtered semitransparent Pt layer. The films grown from the above-mentioned four compositions were 200±30 nm thick. For the study of thickness effects PZT 20/80 films with thickness in the 20–250 nm range were grown using the same procedure.

All the studied PZT/SRO/STO (001) heterostructures dealt with here were subjected to transmission electron microscopy (TEM) investigations. Cross section samples were prepared so that the electron beam was incident onto the samples from the [110] direction. Thorough TEM investigations of the PZT 20/80 films were shown in previous paper.[30] Figure 1 shows the TEM micrographs taken on the cross sections of the samples with PZT 40/60 and PZT 60/40 layers. The dark-contrast wedgelike features exhibited by the PZT 40/60 film are 90° *twin* domains, typical for tetragonal PZT films.[31] From electron diffraction patterns

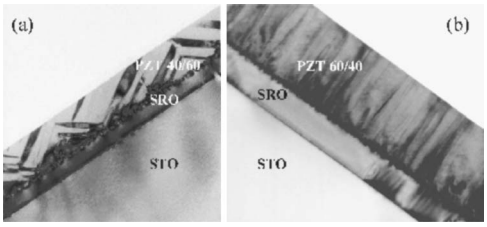

FIG. 1. TEM cross section micrographs seen from [110] direction: (a) PZT 40/60 film grown on $SrRuO_3$-coated $SrTiO_3$ (001) and (b) PZT 60/40 film grown on $SrRuO_3$-coated $SrTiO_3$ (001).

(not shown) the films were found to be epitaxial and the structure of the PZT 40/60 film was determined to be tetragonal while the structure of the PZT 60/40 film was rhombohedral. X-ray diffraction measurements confirmed the epitaxial growth of our PZT/SRO/STO heterostructures. For example, the x-ray diffraction (XRD) (θ-2θ) spectrum acquired on the 215 nm thick epitaxial PZT 20/80 film grown on SRO/STO (001) is given in Fig. 2.

Ferroelectric properties were analyzed by dynamic and static hysteresis measurements using TF2000 analyzer (Aix-ACT). Photocurrent measurements were performed at room temperatures using an experimental setup comprising a grating monochromator (LOT-Oriel MSH101), UV lamp (LOT-Oriel), and an electrometer (Keithley 6517). The light was brought just above the top electrode of the MFM structure using a 1 mm diameter optical fiber. The area of the top electrode was 0.09±0.01 mm^2 and the contacting was performed using micromanipulators equipped with 12 μm diameter tungsten tips in order to ensure a good illumination of the top electrode.

III. EXPERIMENTAL RESULTS

A. The hysteresis loop

Ferroelectric behavior of the PZT films is presented in Fig. 3. We just point out large values of polarization, even for the films with rhombohedral structure, and the sharp switching in the tetragonal phase. The average values of the rem-

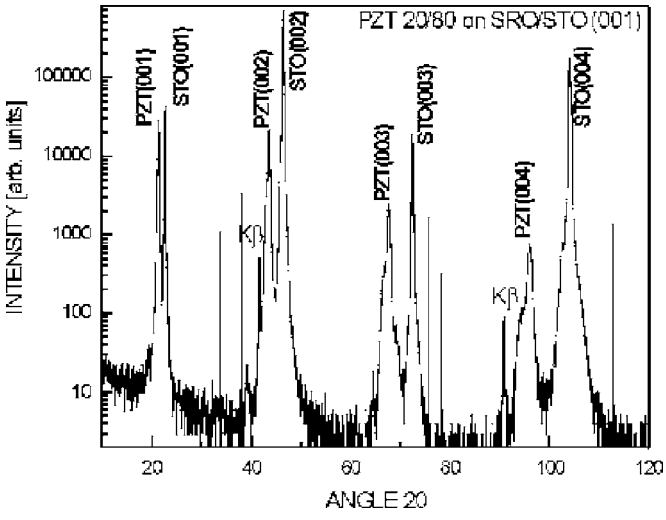

FIG. 2. XRD spectrum of an epitaxial PZT 20/28 film grown on $SrRuO_3$-coated $SrTiO_3$ (001).

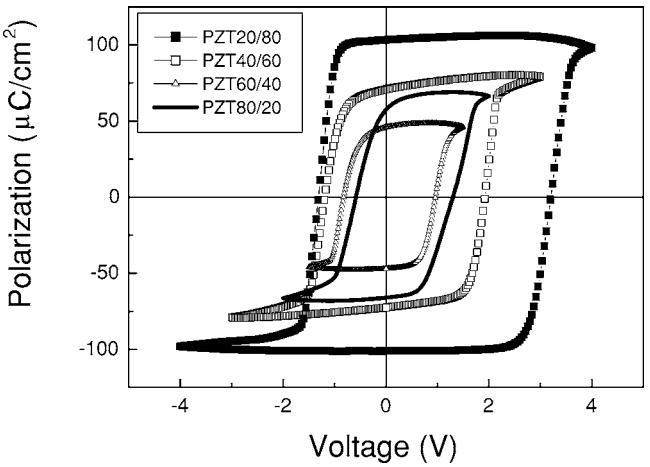

FIG. 3. Dynamic hysteresis loops for SRO-PZT-SRO structures with epitaxial PZT films of different compositions. The loops were recorded using a triangular voltage of 1 kHz frequency.

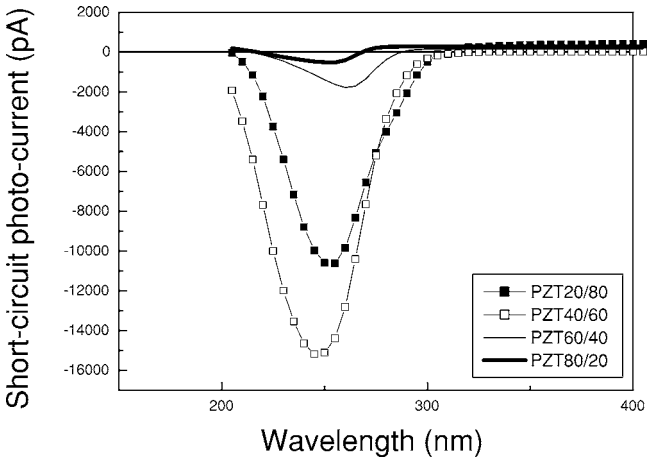

FIG. 4. Wavelength dependence of the short-circuit photocurrent for epitaxial PZT films with different compositions. The recorded current was divided to the magnitude of the incident power and then normalized to the maximum.

nant polarization and coercive field are given in Table I. The remnant polarization has a minimum around the morphotropic phase boundary and the coercive field is smaller in the rhombohedral phase, as reported in the literature.[32–34]

As seen from Fig. 3, all the loops are shifted towards the positive voltage. We remind that the reference electrode for the voltage applied during the hysteresis measurements is the top one. The positive shift is associated with the presence of an internal electric field oriented to the top contact. When the negative polarity of the external voltage is applied on the top electrode the internal field has the same orientation as the external applied field. The consequence is a noticeable reduction of the coercive field, because the polarization switching takes place at a lower voltage than in the absence of the internal field. The opposite is valid for the positive polarity applied on the top electrode. However, this positive shift differs in magnitude from contact to contact, suggesting that it is related to the local distribution of charged defects at the bottom and top interfaces.

B. Spectral distribution of the PHC and evaluation of the band gap for different Zr/Ti ratios

The spectral distributions of the short-circuit PHC are presented in Fig. 4. A significant short-circuit current was detected in the UV region of the electromagnetic spectra, i.e., below 300 nm, for all four PZT compositions. The magnitude of the measured PHC was constantly higher in the case of the films with tetragonal structure. It has to be mentioned that the magnitude of the measured PHC was not the same on different contacts of the film, despite the fact that in every case the optic alignment was performed in such a way to achieve maximum signal under illumination.

The band gap of the PZT films with different compositions can be estimated if the threshold wavelength of the short-circuit photocurrent uses the following equation:

$$E_g(\text{eV}) = \frac{hc}{q\lambda(\mu\text{m})} = \frac{1.24}{\lambda(\mu\text{m})}, \tag{1}$$

where E_g is the band gap, c is the speed of light, h is Planck's constant, q is the electron charge, and λ is the wavelength. Thus, expressing the threshold wavelength in microns makes it easy to evaluate the band gap in eV. The resulting band gap of the four investigated compositions is presented in Fig. 5 as a function of the Zr/Ti ratio. The corresponding threshold wavelength, as extracted from the normalized spectral distribution presented in Fig. 4, is given in a separate column of Table I.

TABLE I. The estimated values of the remnant polarization P_r and coercive field E_c in the case of the four studied PZT compositions. The threshold wavelength used to calculate the band gap using Eq. (1) is shown in the last column.

Sample	P_r (μC/cm^2)	E_c (kV/cm)	Threshold wavelength λ (nm)
PZT20/80	99±5	112	318
PZT40/60	72±5	78	305
PZT60/40	45±5	44	295
PZT80/20	62±5	47	280

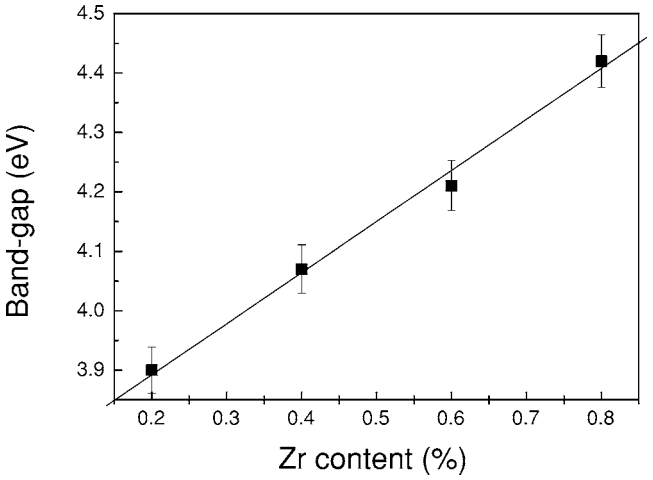

FIG. 5. The variation of the band-gap energy with the Zr content for epitaxial PZT thin films. The band-gap value was calculated using Eq. (1) with the threshold wavelengths shown in Table I.

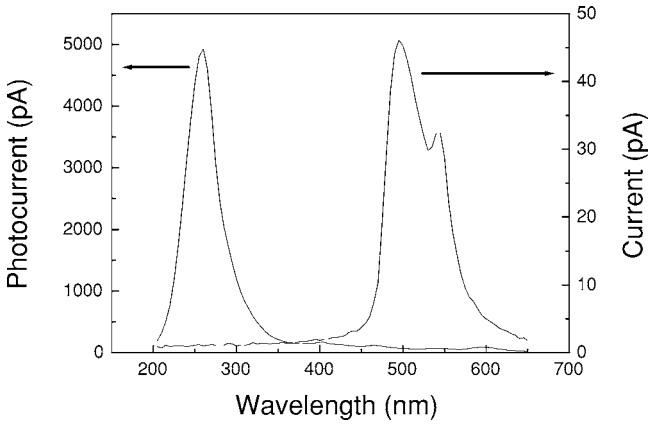

FIG. 6. The PHC signal recorded without (left scale) and with (right scale) the UV cutoff filter.

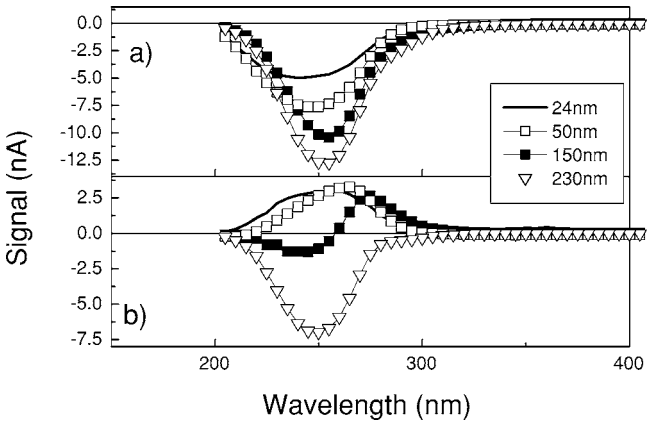

FIG. 7. The thickness dependence of the PHC signal for the two orientations of the polarization: (a) up; (b) down. The polarization is considered "up" when is oriented toward the top SRO electrode.

It can easily be observed from Fig. 5 that the band gap increases with increasing Zr content, as previously reported on polycrystalline films.[14,15,35] The main difference regards the band-gap value which is larger than other experimental reports for all composition.[36] We assume that this is due to the crystalline quality of the epitaxial films. The structural disorder of polycrystalline films smears the edges of the valence and conduction bands, introducing tails of states in the forbidden band similar to those reported on other ferroelectrics.[37] Thus, the band gap determined from optical or photoelectrical methods can be apparently smaller than the intrinsic value.

During the spectral measurements a nonzero signal at wavelengths corresponding to photon energies smaller than the forbidden band of the PZT was observed. In order to confirm this signal at subgap energies spectral distribution was measured using a cutoff filter for the UV range. Therefore, all the light with wavelengths shorter than 500 nm was cut off, preventing the band-to-band generation of charge carriers. As shown in Fig. 6, a clear signal can be observed, although its magnitude is very small compared with the signal due to the fundamental absorption. This subgap signal suggests the presence of occupied states in the forbidden band of PZT. These most probably are deep trapping levels, which release trapped carriers when the energy of the incident photons is equal to the activation energy of the trap.

C. The PHC and the thickness of the PZT film

The largest photoelectric signals were obtained on the PZT 20/80. Therefore, the thickness study was performed on films with this composition. Random electrodes were measured on several samples with thickness in the 20–250 nm range. The results are presented in the Fig. 7 for the two orientations of the ferroelectric polarization. We mention that the polarization values were not very much dependent on thickness, being in all cases around 100 $\mu C/cm^2$.[30]

It is interesting to note that, for one orientation of the polarization, the PHC signal is almost proportional to the thickness of the PZT films. This fact suggests a possible bulk effect. If the photoelectric signal is generated in the bulk of the film it is expected that the signal will increase with increasing thickness. However, looking for the results in the case of the opposite polarization orientation, we see that the apparent thickness dependence disappears. The magnitude of the PHC signal has a random behavior with the thickness in this case. Regarding the change of the sign during the wavelength scan, we cannot make any comment at this moment. It was observed that, for the same thickness, there are contacts on which the PHC changes the sign when polarization changes orientation, which is considered normal behavior;[24] contacts on which PHC changes the sign during the wavelength scan, although the polarization orientation was not changed; and contacts on which PHC does not change the sign after polarization orientation was changed.

Examples of the three situations are given in Fig. 8. These intriguing phenomena require further studies and will not be discussed here. We just notice that the sign of PHC is related to the orientation of the internal electric field respon-

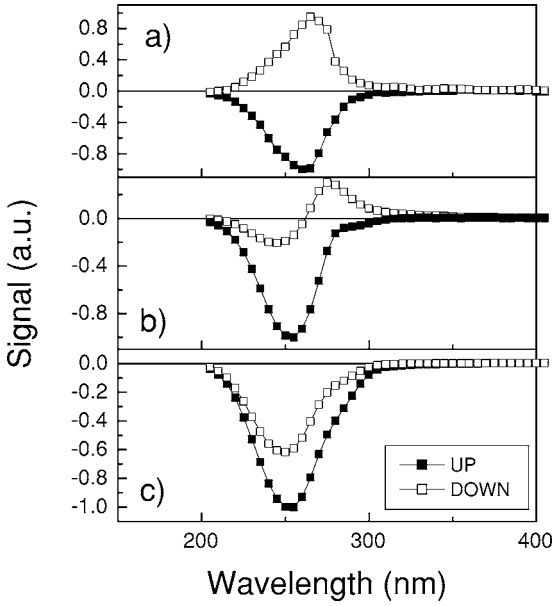

FIG. 8. The three situations encountered when measuring the PHC for the two possible orientations of the ferroelectric polarization, "up" and "down," relative to the top electrode. (a) The current completely changes the sign after polarization switching; (b) the sign changing is only partial; and (c) there is no change in the sign.

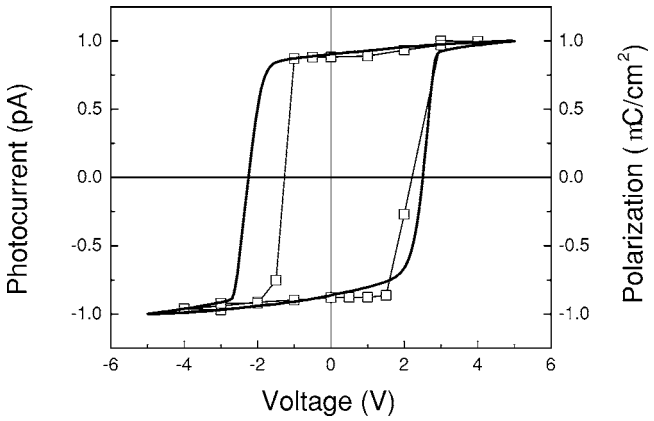

FIG. 9. The behavior of the PHC signal when the ferroelectric polarization describes a full hysteresis loop. Both ferroelectric polarization (measured at 1 kHz) and PHC signal were normalized to their respective maximum value.

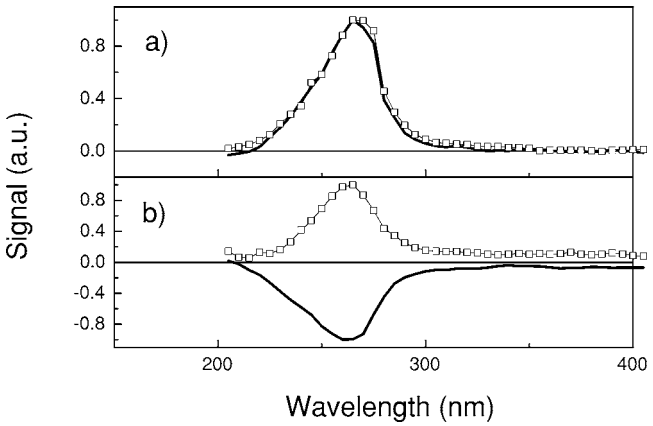

FIG. 10. The PHC signal just after removing the poling field (line) and after 5 days from poling (open squares) (a) for the "down" direction of polarization and (b) for the "up" direction. OC stands for open-circuit conditions.

sible for the occurrence of the short-circuit current. We expect that this field changes the orientation when the polarization changes the orientation. Thus, PHC normally should change sign when the polarization is changed. It is not clear yet why this fact does not happen on every contact. It seems that, for some reason, the orientation of the internal field does not change after poling the film in opposite direction, or it is changing suddenly during the wavelength scan. We can speculate that nonuniform distribution of charged traps might play a role in these phenomena.

D. Relationship between the polarization and photoelectric current

Previous studies on polycrystalline films have suggested that the sign change of PHC with the polarization orientation can be used for the nondestructive reading of polarization state.[24,27] In order to confirm this behavior PHC signal was measured after poling the epitaxial PZT 20/80 films with different voltages aiming to obtain a full hysteresis loop of the ferroelectric polarization. A variable poling voltage, having the reference of the voltage polarity on the top electrode, was applied on the film for 20 s. The spectral distribution of the PHC was measured after removing the poling voltage. The poling voltage was varied for the hysteresis loop having as the starting point the negative saturation of polarization.

The peak value of PHC (measured at about 260 nm wavelength) represented as a function of the poling voltage is shown in Fig. 9 together with the dynamic hysteresis loop. It is important to note that PHC describes exactly the same hysteresis loop as the polarization. Moreover, the hysteresis loop of PHC is almost rectangular with sharp switching and flat saturation polarization for both positive and negative branches. The above result clearly shows that the PHC signal is directly related to the ferroelectric polarization. Moreover, the PHC magnitude depends on the magnitude of the polarization whereas the sign depends on the polarization orientation.

Two other experiments were performed in order to verify if the PHC can be used as a nondestructive reading tool of the polarization state. In the first experiment, the polarization retention was verified. First, the sample was poled "up" (polarization oriented to the top electrode) and the PHC signal was recorded immediately after removing the poling field and after keeping the sample in open circuit for 5 days. The same procedure was applied for the "down" direction of polarization. Figure 10 shows that PHC signal after poling down keeps the same sign after 5 days whereas the opposite direction is not stable. After 5 days of keeping the measured device in open-circuit (OC) conditions most of the initially up polarization was back switched to down direction. Further on, the same experiment was performed keeping the sample in short-circuit (SC) conditions; i.e., the top and bottom electrodes were contacted just after poling and first PHC measurement. Thus, the device was poled up again and kept in SC. The results are presented in the Fig. 11. It can be easily seen that the sign of PHC signal was not changed after keeping the sample in SC conditions. After another 5 days in OC conditions the sign was changed, as the polarization has back switched from up to down direction. This complements the results shown in Fig. 10 and shows that the photocurrent is a nondestructive probing technique for the polarization state.

Finally, the PHC signal was measured after fatigue. Recently it was shown that fatigue can occur, in certain conditions, even in ferroelectric PZT films with SRO top and bot-

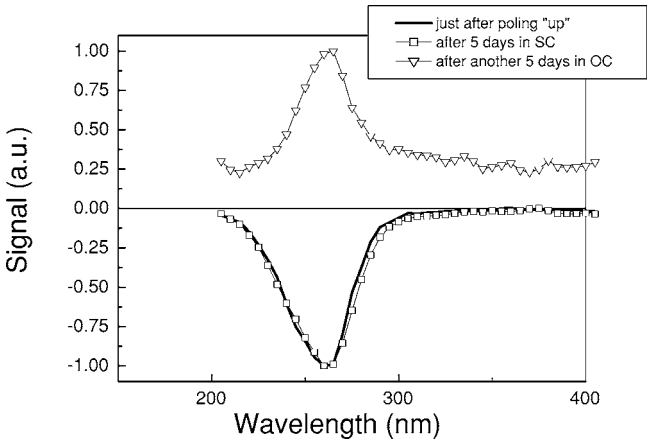

FIG. 11. The PHC signal for the "up" poling after keeping the sample for 5 days in different conditions. SC is for short circuit, while OC is for open circuit.

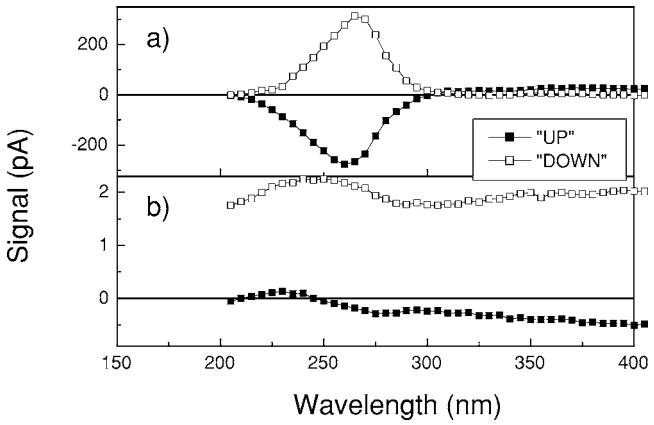

FIG. 12. The PHC signal measured for the "up" and "down" directions of polarization, before and after fatigue with 10^8 cycles. The fatigue was performed with a rectangular signal of 100 kHz frequency and 5 V amplitude.

tom electrodes.[38] Therefore, one ferroelectric capacitor was fatigued by applying 10^8 cycles at a frequency of 100 kHz and 5 V amplitude. The PHC signal was measured for the up and down directions of polarization before and after fatigue. The results are shown in Fig. 12 and the corresponding hysteresis loops before and after fatigue tests are shown in Fig. 13.

From Fig. 13 it can be observed that the polarization decreases about an order of magnitude after fatigue. Correspondingly, the magnitude of the PHC signal is reduced, but more than two orders of magnitude, as can be observed in Fig. 12. This result would suggest a direct relation between polarization and PHC magnitudes, although the results obtained for different Zr/Ti ratios and different thicknesses do not entirely support this conclusion. The relation between polarization and photocurrent appears to be more complex and subjected to important influences from other factors such as internal fields, interface effects, traps, etc.

E. Potential for UV-Vis detection

At the end, we have to notice that in some cases the magnitude of the UV signal at the peak wavelength was as high as 20 nA for a device area of only 0.09 mm^2. Using a calibrated photodiode for the UV domain it was possible to evaluate the incident power and estimate the current responsivity R_I of the PZT, according to the equation

$$R_I = \frac{I}{P_{\text{inc}}}, \tag{2}$$

where I is the measured current and P_{inc} is the incident power on the top electrode surface. Responsivities as high as 1 mA/W can be obtained on the rather defect-free PZT films, i.e., very low density of extended structural defects such as misfit and threading dislocations.[30] This might be an indirect proof that, like in the case of normal semiconductors, in PZT structural defects can act as scattering and trapping centers, reducing both the mobility and the lifetime of the photogenerated carriers and leading to small photoelectric signals. Therefore, by optimizing the microstructure it is possible to obtain PZT films with competitive characteristics for the UV detection.

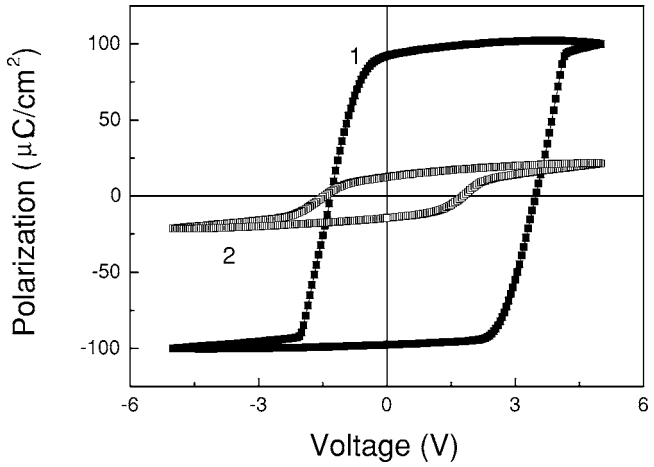

FIG. 13. The hysteresis loops before (1) and after fatigue (2). The 10^8 cycle fatigue was performed with a rectangular signal of 100 kHz frequency and 5 V amplitude.

IV. DISCUSSIONS

As we have pointed out, the main problem is the generation mechanism of the short-circuit photocurrent. It is rather clear that the above results cannot be explained only through the bulk photovoltaic effect observed in the case of ferroelectric single crystals or ceramics. The following facts should be considered.

(i) The films are thin and it can be assumed that the light absorption is rather uniform inside the film.
(ii) The two interfaces are not equivalent, even the bottom and top electrodes are from the same material, just because the two electrodes are usually differently processed.
(iii) It is generally agreed that PZT forms Schottky contacts with electrodes including SRO, thus a nonzero electric field can exist in the region near the metal-ferroelectric interfaces.[39]
(iv) The MFM structure can be represented as a simple back-to-back connection of two Schottky diodes, with a certain neutral volume in between that can be modeled as an ideal capacitor parallel to a leakage resistor, i.e., classical *RC* model.

Considering these, the recently proposed model for the metal-ferroelectric interface can be used to tentatively explain the origin of the short-circuit photovoltaic current.[40] The band diagram of the MFM structure is represented schematically in Fig. 14.

According to the mentioned model the maximum electric field at the interface, in the absence of an external voltage, is given by

$$E_m = \sqrt{\frac{2qN_{\text{eff}}V'_{\text{bi}}}{\varepsilon_0\varepsilon_{\text{st}}}} \pm \frac{P}{\varepsilon_0\varepsilon_{\text{st}}}. \tag{3}$$

N_{eff} is the effective density of the fixed charge situated within the depletion region, considering both the ionized shallow impurities and the charged traps. P is the polarization and ε_{st} is the static dielectric constant. V'_{bi} is the apparent built-in

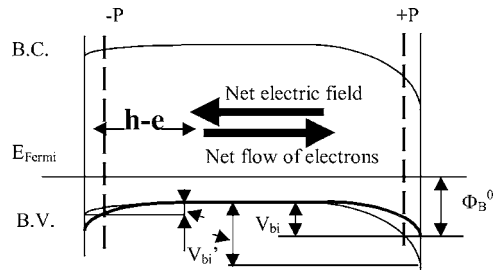

FIG. 14. The schematic band diagram of an epitaxial PZT film with perfectly symmetric electrodes. The PZT was considered as a *p*-type material. BC and BV are for conduction and valence bands, respectively. Φ_B^0 is the potential barrier, V_{bi} is the built-in potential in the absence of polarization, and V'_{bi} is the built-in potential in the presence of the polarization charges.

potential in the presence of the polarization charge near the Schottky interface. As resulting from Fig. 14, the V'_{bi} will be smaller at the interface with negative polarization charge, while at the other interface it will be larger than in the absence of polarization. On the other hand, in Eq. (3) the plus sign is valid at the interface with negative polarization charge, while the minus sign is valid at the interface with positive polarization charge. According to Eq. (3) the field will be higher, in absolute value, at the interface with negative polarization charge.

The important conclusion of Eq. (3) is that the two electrodes are not at the same potential. For a perfect symmetric structure, the same built-in potential at the two interfaces and with no ferroelectric polarization, the maximum electric field at the two interfaces will be the same and the net field inside the structure will be zero. The presence of the ferroelectric polarization breaks the symmetry and makes the two interfaces unbalanced. Therefore, a nonzero net field will exist in the MFM structure. This will be oriented from the interface with positive polarization charge towards the interface with negative polarization charge, as shown in Fig. 14. The short-circuit current generated by film illumination with light having the photon energy equal to or higher than the PZT band-gap energy E_g can now be easily explained. Electron-hole pairs will be generated by fundamental absorption of the incident light. The orientation of the electric fields within the interface regions is such that the photogenerated electrons are expelled towards the neutral volume, while the holes are driven inside the depleted region. A net short-circuit current can occur under illumination, as in any normal Schottky diode. In the case of up polarization a net electron current will flow from the bottom interface (with negative polarization bound charge) toward the top interface (with positive polarization bound charge). The sign of the measured current on the top electrode will be negative. For the down polarization, the electron current will flow in the opposite direction and the sign will be positive. That explains the change of the PHC sign after reversing the polarization orientation.

In an ideal situation the ferroelectric structure, with top and bottom electrodes from the same material, should be perfectly symmetric if the ferroelectric film is single crystal and single domain and if the two interfaces are equivalent. The PHC signal will change the sign in this case, when the polarization orientation is changed, and the spectral distributions will be similar for the two orientations, as shown in Fig. 8(a). A nonhomogeneous distribution of structural defects, either in the bulk or near the two electrode interfaces, can alter the above-mentioned ideal structure. Such defects can act as trapping centers, becoming charged. The nonuniform distribution will induce other internal fields, adding to the field shown in Fig. 14 and affecting the polarization switching by pinning domains or by inducing back switching after removal of the poling field. If the back switching is dominant, then the polarization will not change the orientation and the PHC will have the same sign, as shown in Fig. 8(c). Some of the charged centers can be "erased" during the scan if the energy of the incident photons is enough to excite the trapped carrier back into the conduction or valence band. This process will lead to a change in the magnitude and direction of the total internal field during the scan. Consequently, there can be sudden changes in the sign of the PHC signal, as shown in the Fig. 8(b).

These more complicated situations might be related to the polarization imprint and switching kinetics. As the PHC measurement is a zero-field measurement and as it gives information on the polarization magnitude and direction without applying an external field, it can be better used in studying such effects, in which external applied field might be detrimental. A detailed study of the effect of the imprint on the photoelectric current is currently performed and will be published elsewhere.

V. CONCLUSIONS

Photoelectric effects have been studied on epitaxial PZT films. This study had revealed the following.

(i) The PHC signal is directly related to the orientation of the ferroelectric polarization and it is apparently dependent on polarization magnitude as well.
(ii) Local microstructure affects the PHC behavior through the ferroelectric polarization.
(iii) The PHC can be used as a nondestructive readout of the ferroelectric nonvolatile memories, subject to the fact that the film is free of imprint in any point and is kept in short-circuit conditions.
(iv) The PHC has large values in the epitaxial PZT films, up to a current responsivity of 1 mA/W at the peak wavelength of the spectral distribution. This makes the epitaxial PZT films suitable for solid-state UV detectors.
(v) The band-gap energies evaluated from the PHC spectral distribution for different PZT compositions range from 3.9 to 4.4 eV and it is constantly higher than the reported experimental values on polycrystalline films, but agree well with theoretical values.

Correlated with PFM the PHC signal can be a powerful tool to extract information about the state of polarization, imprint, local bias fields, and retention.

ACKNOWLEDGMENTS

This work was partly supported by the Volkswagen Stiftung under Contract No. I/77738 and by the CEEX program

(Romanian Ministry of Education and Research) under Project No. DINAFER–2–CEEX–06–11–44. The authors are also thankful to Professor Dietrich Hesse for the TEM investigation and to Xenia Boldyreva for the XRD characterization.

[1]S. M. Sze, *Physics of Semiconductor Devices*, 2nd ed. (Wiley, New York, 1981).
[2]M. E. Lines and A. M. Glass, *Principles and Applications of Ferroelectrics and Related Materials* (Clarendon, Oxford, 1977).
[3]V. M. Fridkin, *Photoferroelectrics* (Springer-Verlag, Berlin, 1979).
[4]A. M. Glass, D. von der Linde, and T. J. Negran, Appl. Phys. Lett. **25**, 233 (1974).
[5]P. S. Brody, Appl. Phys. Lett. **38**, 153 (1981).
[6]S. B. Lang and E. H. Putley, Appl. Opt. **21**, 2304 (1982).
[7]R. Watton, Ferroelectrics **133**, 5 (1992).
[8]R. W. Whatmore and R. Watton, Ferroelectrics **236**, 259 (2000).
[9]S. G. Porter, Ferroelectrics **33**, 193 (1981).
[10]L. Pintilie, M. Alexe, I. Pintilie, and T. Botila, Appl. Phys. Lett. **69**, 1571 (1996).
[11]A. G. Chynoweth, Phys. Rev. **102**, 705 (1956).
[12]F. S. Chen, J. Appl. Phys. **40**, 3389 (1969).
[13]M. Simon, St. Wevering, K. Buse, and E. Ktraetzig, J. Phys. D **30**, 144 (1997).
[14]J. Robertson, W. L. Warren, and B. A. Tuttle, J. Appl. Phys. **77**, 3975 (1995).
[15]S. Yang, Y. Zhang, and D. Mo, Mater. Sci. Eng., B **127**, 117 (2006).
[16]G. Chanussot, Ferroelectrics **20**, 37 (1978).
[17]W. Kraut and R. von Baltz, Phys. Rev. B **19**, 1548 (1979).
[18]P. S. Brody, J. Solid State Chem. **12**, 193 (1975).
[19]S. R. Kim and S. K. Choi, Ferroelectr., Lett. Sect. **31**, 63 (2004).
[20]K. Nonaka, M. Akiyama, T. Hagio, and A. Takase, J. Eur. Ceram. Soc. **19**, 1143 (1999).
[21]W. L. Warren, D. Dimos, B. A. Tuttle, R. D. Nasby, and G. E. Pike, Appl. Phys. Lett. **65**, 1018 (1994).
[22]W. L. Warren, D. Dimos, B. A. Tuttle, G. E. Pike, R. W. Schwartz, P. J. Clews, and D. C. McIntyre, J. Appl. Phys. **77**, 6695 (1995).
[23]A. L. Kholkin, S. O. Iakovlev, and J. L. Baptista, Appl. Phys. Lett. **79**, 2055 (2001).
[24]A. Kholkin, O. Boiarkine, and N. Setter, Appl. Phys. Lett. **72**, 130 (1998).
[25]S. Thakoor and J. Maserjian, J. Vac. Sci. Technol. A **12**, 295 (1994).
[26]J. Lee, S. Esayan, J. Prohaska, and A. Safari, J. Appl. Phys. **64**, 294 (1994).
[27]S. Thakoor, Appl. Phys. Lett. **60**, 3319 (1992).
[28]S. Thakoor, Appl. Phys. Lett. **63**, 3233 (1993).
[29]Y. S. Yang, S. J. Lee, S. Yi, B. G. Chae, S. H. Lee, H. J. Joo, and M. S. Jang, Appl. Phys. Lett. **76**, 774 (2000).
[30]I. Vrejoiu, G. Le Rhun, L. Pintilie, D. Hesse, M. Alexe, and U. Goesele, Adv. Mater. (Weinheim, Ger.) **18**, 1657 (2006).
[31]I. Vrejoiu, G. Le Rhun, N. D. Zakharov, D. Hesse, L. Pintilie, and M. Alexe, Philos. Mag. **86**, 4477 (2006).
[32]C. M. Foster, G. R. Bai, R. Csencsits, J. Vetrone, R. Jammy, L. A. Wills, E. Carr, and J. Amanao, J. Appl. Phys. **81**, 2349 (1997).
[33]M. Klee, R. Eusemann, R. Waser, W. Brand, and H. van Hal, J. Appl. Phys. **72**, 1566 (1992).
[34]S. Yokoyama *et al.*, J. Appl. Phys. **98**, 094106 (2005).
[35]H. Lee *et al.*, J. Appl. Phys. **98**, 094108 (2005).
[36]C. H. Peng, J. F. Chang, and S. B. Desu, Mater. Res. Soc. Symp. Proc. **243**, 21 (1992).
[37]B. Dulieu, J. Bullot, J. Wery, M. Richard, and L. Brohan, Phys. Rev. B **53**, 10641 (1996).
[38]L. Pintilie, I. Vrejoiu, D. Hesse, and M. Alexe, Appl. Phys. Lett. **88**, 102908 (2006).
[39]I. Stolichnov, A. Tagantsev, N. Setter, J. S. Cross, and M. Tsukada, Appl. Phys. Lett. **75**, 1790 (1999).
[40]L. Pintilie, I. Boerasu, M. J. M. Gomes, T. Zhao, R. Ramesh, and M. Alexe, J. Appl. Phys. **98**, 124104 (2005).